Frequency-Dependent Signal Blind Area "Cavity" in Multi-Layer Optical Waveguide

Yao Guozheng Liu Ying

(*Fundamental Department*, *Academy of Armored Forces Engineering*, *Beijing* 100072, *China*)

Abstract Because the size of photonic device is close to the size of optical wavelength, photonic circuit shows significant diffractive characteristics, which can be used to design photonic devices with novel function. To realize the similar "skin effect" of electronic circuit, we utilize the similarity between "Schrödinger Equation" and the wave function in inhomogeneous medium, and design a type of multi-layer cylindrical optical waveguide with high gradient refractive index and pseudo-gravity potential index distribution. Simulation shows high frequency signal propagate in the surface layer, and signal blind area ("cavity") exists in the inner part of the waveguide. The size of the cavity varies with the wavelength of the light. The boundary of the cavity locates near the inner-boundary of the layers. Longer wave is less affected by the discontinuity, and can penetrate further into the inner material. The domain of the cavity decreases with the wavelength. This result may have significance for the design of "perfect invisible cloak" and new type photonic circuit.

Key words materials; optical wave guide; photonic device; diffraction; signal blind area; cavity

OCIS codes 160.5140; 220.2560; 230.3240

多层结构光波导中依赖于频率的信号盲区

姚国政 刘 影

(装甲兵工程学院基础部，北京 100072)

摘要 由于光子回路中光子器件尺寸和光波长相当，所以衍射现象比较明显，据此可以实现类似于电路中的趋肤效应。根据光信号在介质中的传播方程和薛定谔方程的相似性，设计了一种多层柱状结构光波导，高频光信号沿着波导表层传播，其内部存在信号盲区。仿真计算表明：盲区随信号频率的增大而增大。盲区的边界通常位于多层介质的内分界面上。较高的折射率梯度和类似于引力势的折射率分布有利于形成信号盲区。该结果有助于隐身衣或新型光子回路的设计。

关键词 材料；光波导；光子器件；衍射；信号盲区；空腔

中图分类号 TN252 **文献标识码** A **doi**：10.3788/CJL201441.s106002

1 Introduction

With the rapid development of photon-electronic technology, photonic circuits may play a main role in the next-generation optical networks and optical interconnects for its higher performance, lower package and lower power consumption[1-3]. Because the size of the photonic device is close to that of the optical wavelength[4-6], photonic circuit shows more diffractive characteristic compared with the traditional electronic circuits. We can utilize "diffraction" to design new photonic devices.

收稿日期：2013-10-20；**收到修改稿日期**：2013-11-14

基金项目：装甲兵工程学院创新基金

作者简介：姚国政(1971—)，男，博士，讲师，主要从事光子信息方面的研究。E-mail：yaoguozheng@163.com

2 Waveguide with high gradient refractive index and pseudo-gravity potential index distribution

Diffraction occurs when the light meets obstacles. If a clump of another medium is embedded in a uniform background, the light may travel around , or penetrate into the embedded medium. In the embedded object, the domain and the amplitude of the diffractive wave vary with the boundary of the medium and the wavelength of the light. Signal blind area, or "cavity" area, may form. We intend to design a new kind of photonic waveguide, hoping that in some cases, the light will travel through the outer wall of waveguide, leaving the inner space ("cavity") untouched. In other cases, the light signal will penetrate into the inner space and may have further interaction with the inner photonic devices (in case they are placed in).

This can be realized by the multilayer structure waveguide with gradient index. "Gradient index photonic devices" have become a hot topic with the development of transformation optics[7-8]. Discontinuities are allowed along transformation media boundaries and gradient index materials can be designed and readily integrated into photonic circuits [9].

To confine the trajectory of light close to ellipse, which is favorable for the cavity forming, the shape of the layer may be spherical shell or cylinder. Here, for simplicity, we discuss the cylinder multilayer structure in 2D case.

For optical wave with given frequency ν or wave number k, its wave function Ψ should satisfy [10]

$$(\partial_x^2 + \partial_y^2 + n^2 k^2)\Psi = 0. \tag{1}$$

If we set

$$n^2 = R/r - 1, \tag{2}$$

Eq.(1) changes to

$$\left[\partial_x^2 + \partial_y^2 + \left(\frac{R}{r} - 1\right)k^2\right]\Psi = 0. \tag{3}$$

Multiplying it by $-\frac{1}{2m}$, where m means the mass of a given particle, Eq.(3) becomes

$$\left[-\frac{1}{2m}(\partial_x^2 + \partial_y^2) + \left(-\frac{1}{2m}\frac{R}{r}\right)k^2\right]\Psi = -\frac{1}{2m}k^2\Psi. \tag{4}$$

Eq.(4) has the form of Schrödinger Equation

$$\left[-\frac{1}{2m}\nabla^2 + U(r)\right]\Psi = E\Psi. \tag{5}$$

Here, $E = -\frac{1}{2m}k^2 < 0$ and $U(r) = \left(-\frac{1}{2m}\frac{R}{r}\right)k^2$, which is analogous to the gravity potential. In classical cases, the orbit of such a particle is elliptical. So the trajectory of the light should be elliptical.

Near the boundary between the layers, there is a discontinuity of refractive index, where the light exists both the reflection and refraction. The reflection amplitude and transmissive amplitude vary with gradient of the medium and the wavelength of the light. The larger the discontinuity of the index, the easier it is to form the "cavity". The size of the cavity varies with the wavelength of the light. The long wave is less affected by the discontinuity, and can penetrate further into the next material. So the domain of the cavity should decrease with the variety of wavelength.

3 Simulation

Here, the index distribution is based on $n(r)^2 = \frac{R}{r} - 1$. We set $R = 10$ μm, the thickness of each layer is 1 μm, and their middle lines locate at r = 9, 8, 7, 6, 5, 4, 3, 2 μm, respectively. To enhance the gradient of the index, we set $n = 10\sqrt{R/r-1}$. The size of the wafer is set as 25 μm×25 μm, $n = 3$. The distribution of the medium index is shown in Table 1, and its 2D structure is shown in Fig.1.

Table 1 Material profile: refractive index versus cylinder radius

r /μm	9	8	7	6	5	4	3	2
n	3.16	5.00	6.56	8.20	10.0	12.3	15.3	20.0

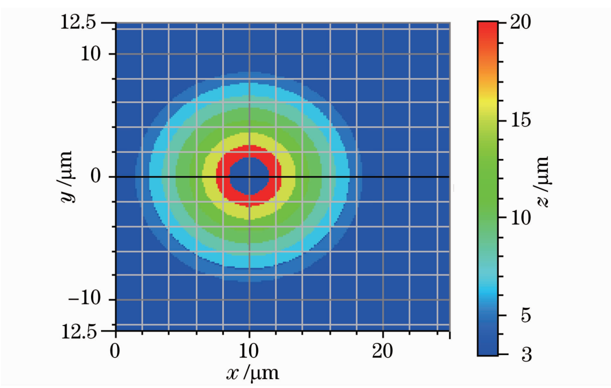

Fig.1 Refraction index profile, the center of waveguide is set at (10,0)

We use the plane source and point source to generate signals, which are placed at the edge of outermost layer. The wavelength of the sources is 3.0, 2.0, 1.5, 1.3, 1.2 μm. The software Optiwave is used for the simulation. The boundary condition is APML, and step size is 0.05 μm.

Results show that no matter which source is adopted, there is a signal blind area near the center. Its boundary always locates at the inner boundary of the

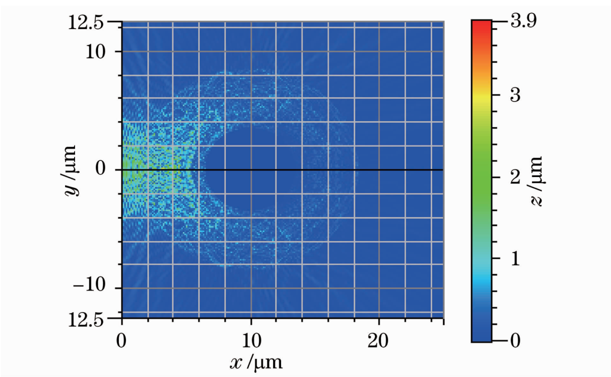

Fig.2 Plane source (at left) case, with transverse type of Gaussian, half-width of 3 μm wavelength of 1.5 μm. The center is set at (10, 0). The diameter of the blind area is about 7 μm

layer. The size of the signal blind area decreases with the wavelength. The simulation results are shown in Table 2 and Figs. 2～4.

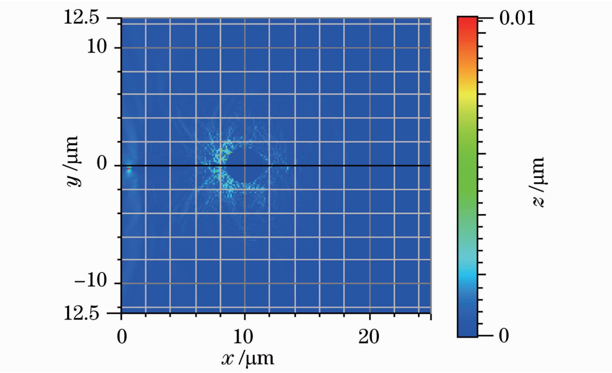

Fig. 3 Point source (at left) case, with wavelength of 3.0 μm. The center is set at (10, 0). The diameter of the blind area is about 3 μm

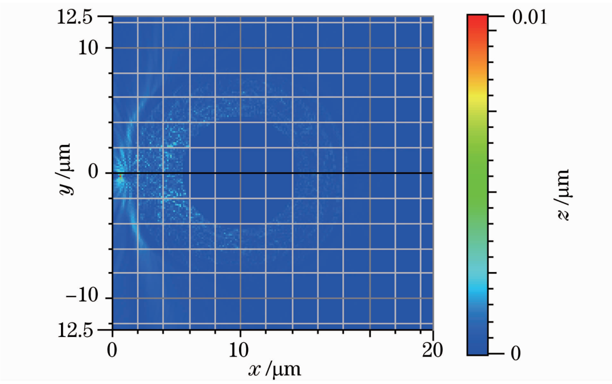

Fig. 4 Point source (at left) case, with wavelength of 1.2 μm. The center is set at (10, 0). The diameter of the blind area is about 9 μm

Table 2 Size of blind area versus wavelength

Diameter of blind area /μm	Wavelength /μm
3.0	3.0
5.0	2.0
7.0	1.5
9.0	1.3
9.0	1.2

4 Conclusion

A kind of multilayer waveguide with high gradient refractive index and pseudo-gravity potential index distribution is proposed. Signal blind area (or "cavity" area) exists when the light travels along it. The location and the size of the cavity depend on the wavelength and gradient of the refraction index. When photonic devices are placed in the center of such a waveguide, for short wavelength light, the devices might remain untouched and keep slept. But for long wavelength light, they may be activated and do something. In the first case, we can say the light travels around the kennel area and moves on. This is a kind of "invisibility" function[11-13], which may have very important significance for "perfect invisibility".

Reference

1 Welch D F, Kish F A, Melle S, *et al*.. Large-scale InP photonic integrated circuits: enabling efficient scaling of optical transport networks[J]. IEEE J Select Top Quantum Electron, 2007, 13(1): 22-31.

2 Nicholes S C, Mašsanovic M L, Jevremovic B, *et al*.. An 838 InP monolithic tunable optical router (motor) packet forwarding chip [J]. J Lightwave Technol, 2010, 28(4): 641-650.

3 Liang D, Bowers J E. Photonic integration: Si or InP substrates [J]. Electron Lett, 2009, 45(12): 578-581.

4 Djavid, F Monifi, A Ghaffari, *et al*.. A photonic crystal L-shaped bend based on ring resonators[J]. Chin Opt Lett, 2008, 6(10): 713-714.

5 Jalali B, Fathpour S. Silicon photonics[J]. J Lightwave Technol, 2006, 24(12): 4600-4615.

6 Komatsu M, Saitoh K, Koshiba M. Design of miniaturized silicon wire and slot waveguide polarization splitter based on a resonant tunneling[J]. Opt Express, 2009, 17(21): 19225-19233.

7 Pendry J B, Schurig D, Smith D R. Controlling electromagnetic fields[J]. Science, 2006, 312(5781): 1780-1782.

8 Leonhardt U. Optical conformal mapping[J]. Science, 2006, 312(5781): 1777-1780.

9 Qi Wu, Jeremiah P Turpin, Douglas H Werner. Integrated photonic systems based on transformation optics enabled gradient index devices[J]. Light: Science & Applications, 2012, 1, e38; doi:10.1038/lso.2012.38

10 Born M, Wolf E. Principles of Optics: Electromagnetic Theory of Propagation, Interference and Diffraction of Light[M]. 7th Expanded ed. Cambridge/New York: Cambridge University Press, 1999.

11 Rahm M, Schurig D, Roberts D A, *et al*.. Design of electromagnetic cloaks and concentrators using form-invariant coordinate transformations of Maxwell's equations[J]. Photon Nanostruct—Fundam Appl, 2007, 6(1): 87-95.

12 Schurig D, Mock J J, Justice B J, *et al*.. Metamaterial electromagnetic cloak at microwave frequencies[J]. Science, 2006, 314(5801): 977-980.

13 Ma H F, Cui T J. Three-dimensional broadband and broad-angle transformation-optics lens[J]. Nat. Commun., 2010, 1(8), doi: 10.1038/ncomms1126, acticle: 124

栏目编辑：殷建芳